Cancer Cell, Volume *33*

Supplemental Information

GKAP Acts as a Genetic Modulator of NMDAR Signaling to Govern Invasive Tumor Growth

Leanne Li, Qiqun Zeng, Arjun Bhutkar, José A. Galván, Eva Karamitopoulou, Daan Noordermeer, Mei-Wen Peng, Alessandra Piersigilli, Aurel Perren, Inti Zlobec, Hugh Robinson, M. Luisa Iruela-Arispe, and Douglas Hanahan

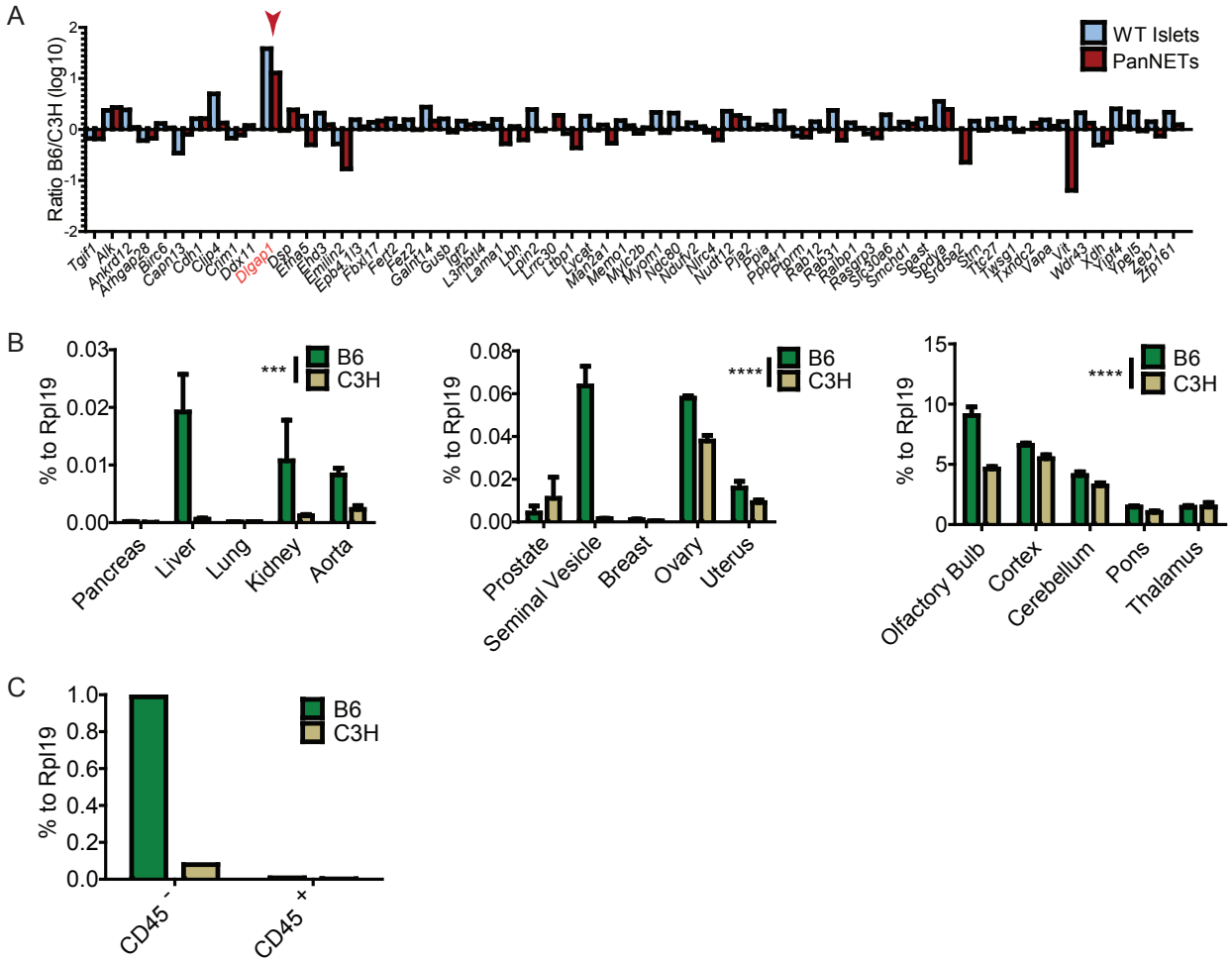

Figure S1. Related to Figure 1.

(A) Re-evaluation of the qRT-PCR data from Chun et al. (Chun et al., 2010). The Y-axis indicates the log of the relative expression ratio in B6 compared to C3H tumors and normal pancreatic islets (B6/C3H). Therefore, a positive value indicates high expression in the B6 background, whereas a negative value indicates the opposite. Red arrowhead denotes *Dlgap1* expression levels.

(B) qRT-PCR comparative analysis of *Dlgap1* mRNA in organs from wild-type C57Bl/6 (B6) and C3Heb/Fe (C3H) mouse strains. Two-way ANOVA with Bonferroni multiple comparisons test. Mean with SEM. ***: $p < 0.001$, ****: $p < 0.0001$. (n = 4-7 mice per analysis). Note that in the case of the pancreas RNA was extracted from whole tissue, which is predominantly composed of pancreatic acinar cells.

(C) qRT-PCR analysis of flow cytometry-sorted populations from B6 and C3H PanNETs. (For each genetic background two mice were used, all tumors were removed from each of the pancreas and cell populations were subsequently sorted to generate the RNA pools used in this qRT-PCR.)

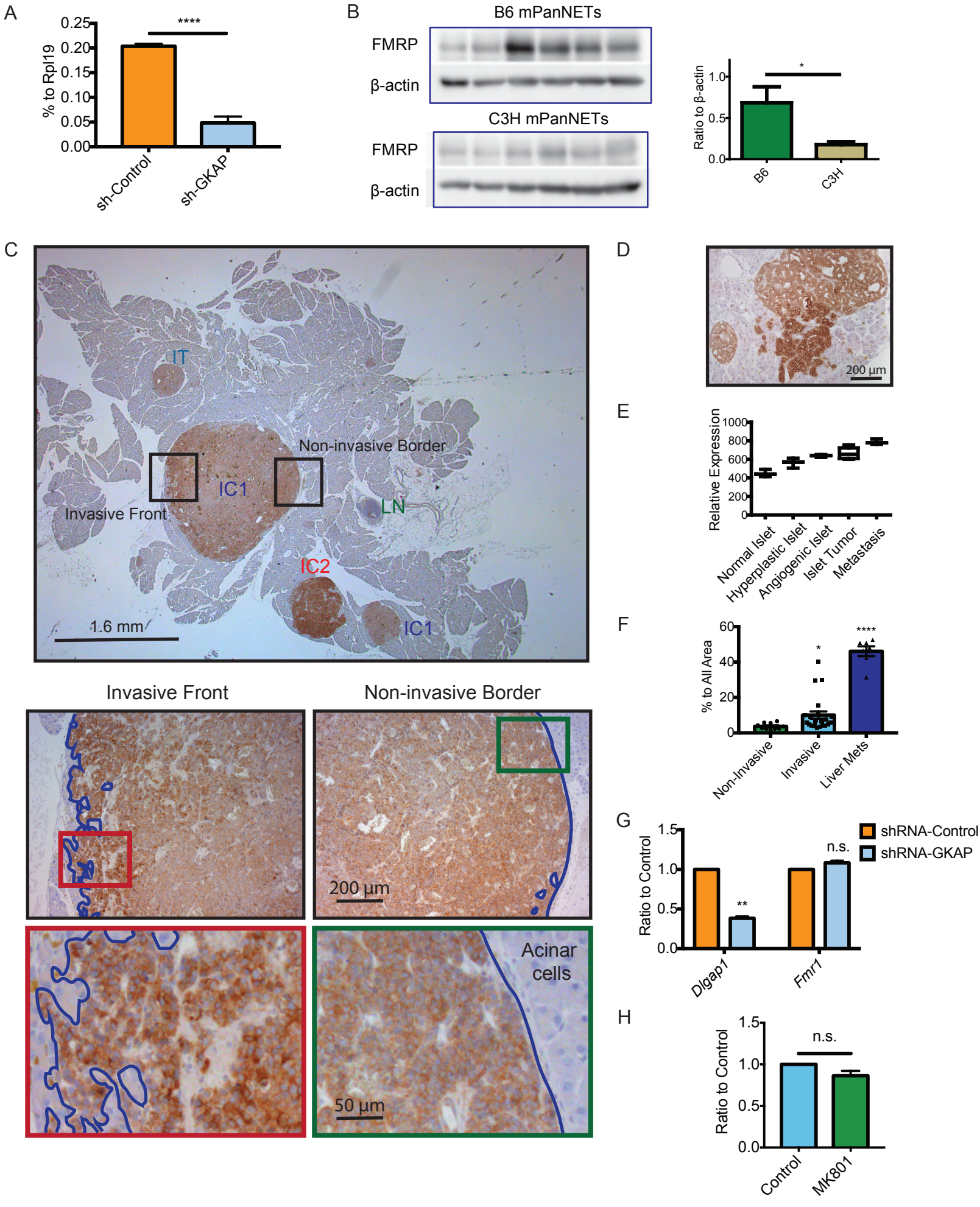
A
% to Rpl19
0.25
0.20
0.15
0.10
0.05
0.00
****
sh-Control
sh-GKAP
B
B6 mPanNETs
FMRP
β-actin
C3H mPanNETs
FMRP
β-actin
Ratio to β-actin
1.0
0.5
0.0
*
B6
C3H
C
IT
Non-invasive Border
IC1
Invasive Front
LN
IC2
IC1
1.6 mm
Invasive Front
Non-invasive Border
200 μm
Acinar cells
50 μm
D
200 μm
E
Relative Expression
1000
800
600
400
200
0
Normal Islet
Hyperplastic Islet
Angiogenic Islet
Islet Tumor
Metastasis
F
% to All Area
60
40
20
0
*
****
Non-Invasive
Invasive
Liver Mets
G
Ratio to Control
1.5
1.0
0.5
0.0
**
n.s.
shRNA-Control
shRNA-GKAP
Dlgap1
Fmr1
H
Ratio to Control
1.5
1.0
0.5
0.0
n.s.
Control
MK801

Figure S2. Related to Figure 4.

(A) qRT-PCR in βTC-3 cells. (n=3 technical controls for qRT-PCR; 2 independent knockdowns were generated, with similar trend. ****: p<0.0001. Unpaired t-test. Mean ± SEM.)

(B) Western blot analysis for FMRP in B6 and C3H PanNETs. Mann-Whitney test, *: p<0.05. (Mean ± SEM. Each lane shows one tumor pool from one mouse, consisting of more than 3 tumors/pool, and 6 mice/group.)(Western blot image was taken from samples ran on the same gel and visualized on the same membrane, and cut by PhotoShop into two images to fit into the figure.)

(C) IHC staining of FMRP in B6 PanNETs. Upper panel: Overview of the whole pancreas. Lower panels: From the same tumor (the IC1 tumor in the center), close-up of FMRP staining at the invasive front (left panels) and at the non-invasive border (right panels). LN: lymph node; IT: islet tumor; IC1: invasive carcinoma type 1 (focally invasive); IC2: invasive carcinoma type 2 (highly invasive). For more details of the grading and definition, see (Chun et al., 2010; Lopez and Hanahan, 2002).

(D) IHC staining of FMRP in a hyperinvasive B6 PanNET observed after sunitinib treatment (Paez-Ribes et al., 2009).

(E) Expression of *Fmr1* in B6 PanNETs throughout the multistage tumorigenesis process, as revealed by microarray (Sadanandam et al., 2015). The box marks the 25th to 75th percentiles, and the whiskers show min to max. The line in the middle of the box indicates the median. No data point is beyond the limit of lines. Normal/hyperplastic/angiogenic islet: n = 3 individual pools; islet tumor: n = 5 individual tumors; metastasis: n = 3 individual liver-metastatic tumors.

(F) IHC quantification of FMRP staining was performed in 10 images of non-invasive tumors, 23 images of invasive tumors and 7 images from metastatic lesion. (Mean ± SEM. *: $p < 0.05$, ****: $p < 0.0001$. 1-way ANOVA, Kruskal-Wallis test, compared to non-invasive tumors.)

(G) qRT-PCR for *Fmr1* and *Dlgap1* transcripts after shRNA knockdown of *Dlgap1* in βTC-3. (Mean ± SEM. Expression levels normalised to shRNA-control. One column statistics, comparing with a hypothetical value of 1. **: $p < 0.01$; n.s.: not significant. N = 3 independent RNA extraction/condition.)

(H) qRT-PCR for *Fmr1* transcripts after MK801 treatment in βTC-3. Expression levels were normalized to PBS-treated control. (Mean ± SEM. One column statistics, comparing with a hypothetical value of 1. n.s.: not significant. N = 3 independent RNA extraction/condition.)

A

Gene	Isoform	FDR	Fold Change (B6/C3H)
Dlgap1	NM_001128180	0	75.21
Dlgap1	NM_027712	0	32.64
Dlgap1	NM_177639	0	36.21

B

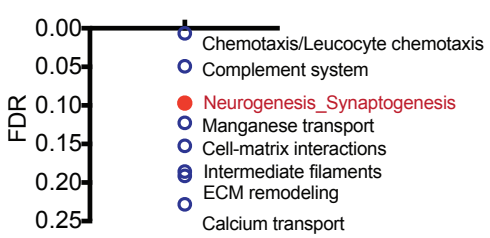

Figure S3. Related to Figure 7.

(A) Isoform analysis for *Dlgap1* protein-coding isoforms using the RNA-seq data from B6/C3H PanNETs.

(B) Gene ontology analysis for genes within the "NMDAR-pathway^{low} signature". GeneGo Metacore software (Thomson Reuters, https://portal.*genego*.com/)

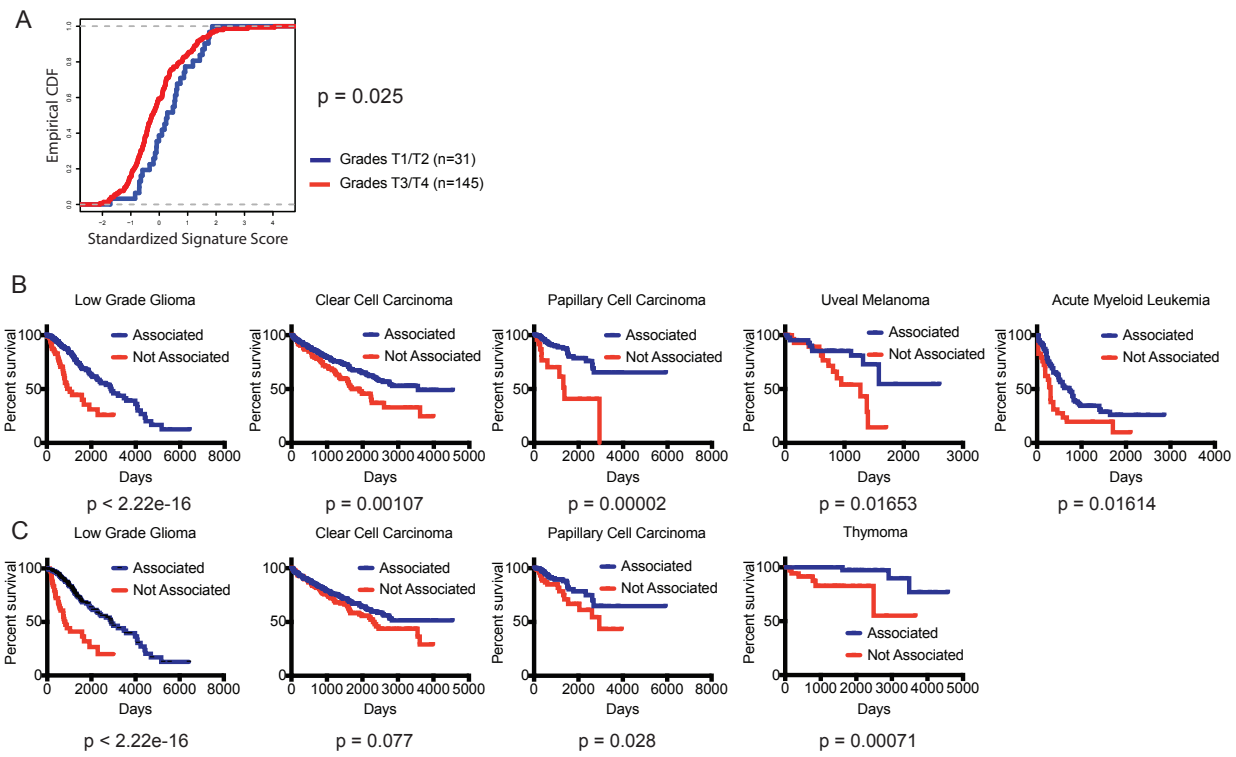

Figure S4. Related to Figure 8.

(A) Empirical CDF plot demonstrating the association of low grade (T1/T2) tumors (marked in blue) and high grade (T3/T4) tumors (marked in red) with "MK801 treatment signature" in PDAC patients. (Using genes with |Z|>4, and log2 fold change (MK801/control) > 1. Kolmogorov-Smirnov test.)

(B) Kaplan-Meier plots showing overall survival in various cancer types from the TCGA (http://cancergenome.nih.gov/). Gene expression data from patient cohorts was stratified by their enrichment for the "MK801 treatment signature" identified in the mPanNET RNA-seq analysis (Figure 7C). Red line: patients whose tumors had gene expression most correlated with the MK801 treatment signature (defined by the top 3.5 Z score). Blue line: patients whose tumors had gene expression least correlated with the MK801 treatment signature (defined by the bottom 3.5 Z score). All patients were included in each cancer type shown, regardless of treatment and staging.

(C) Kaplan-Meier plots showing overall survival in various cancer types from the TCGA (http://cancergenome.nih.gov/). Gene expression data from patient cohorts was stratified by their enrichment for the "NMDAR-pathway^{low} signature" identified in the mPanNET RNA-seq analysis (Figure 7E). Red line: patients whose tumors had gene expression most correlated with the NMDAR-pathway^{low} signature (defined by the top 3.5 Z score); blue line: patients whose tumors had gene expression least correlated with the core driver gene signature (defined by the bottom 3.5 Z score). All patients were included in each cancer type shown, regardless of treatment and staging.